

# DEVELOPMENT OF AN AEROELASTIC METHOD FOR PREDICTING ROTOR AIRLOADS AND STRUCTURAL LOADS

J.C. Su and F. Zhang

Institute for Aerospace Research, National Research Council Canada

**Keywords:** *aeroelasticity, aerodynamics, helicopter rotor, vibration*

## Abstract

The Computational fluid dynamics (CFD) solver, Cobalt, is used with a blade element model imbedded for the aerodynamic inflow prediction of a helicopter rotor. The elastic structural dynamics of the rotor is studied using a multibody dynamics analysis tool, DYMORE, which uses a finite element based multibody dynamics approach for the analysis of nonlinear elastic multibody systems. In this paper, the developed integrated aeroelastic method is applied to the H-34 helicopter rotor which has been flight tested and widely used for rotor model validations. A low speed case with advance ratio  $\mu=0.129$  and rotor thrust coefficient  $C_T/\sigma=0.075$  ( $\sigma$  is solidity of the rotor), and a high speed case with advance ratio  $\mu=0.30$  and rotor thrust coefficient  $C_T/\sigma=0.06$ , are calculated and discussed. The comparison of the computed aerodynamic and structural dynamic results with flight test data showed that the current CFD inflow method gives reasonable predictions for the aerodynamic performance and dynamic response of the rotor and has the potential to be used for more complex practical situations such as a helicopter hovering in the airwake of a ship.

## 1 Introduction

Helicopter rotor loads and vibration have been crucial issues since the beginning of the helicopter industry. Consistently and accurately predicting rotor airloads and structural loads is still very challenging because of strong interactions between rotor aerodynamics and structural dynamics, and complex flow

phenomena around the rotor in most flight conditions. The traditional 2D blade element aerodynamic method has been widely used for rotor aerodynamic analysis and design and has been coupled with structural dynamics in many comprehensive analysis tools [1-3]. For such a method, an aerodynamic look-up table is required and generally inflow and dynamic stall models are also required. In recent years, increasing research has been pursued on three dimensional CFD/computational structural dynamics (CSD) loose and strong couplings [4-5]. With the fast advance in computer memory and speed, this frontier approach is gaining more momentum and is expected to reach an industrial standard for the design of a helicopter soon. However, traditional 2D aerodynamic approaches will continue to serve for most helicopter designs since the two dimensional assumption is a reasonable approximation for rotor blade aerodynamics in most cases. In many situations, the rotor aerodynamic loads are basically spanwise independent, except for the local effects near the blade tip, and thus can be treated on a two dimensional basis due to the use of rotor blades with quite high aspect ratios (the ratio of blade radius to average chord is often 10 or more). The assumption of two dimensionality is further justified by the observation that with increased unsteadiness, the relative effects of spanwise propagations of disturbances, i.e. three dimensionality, are further diminished [6]. Thus, the crucial job when using the aerodynamic blade element method is to provide accurate aerodynamic look-up tables for lift, drag and pitching moment coefficients as well as a correct inflow

condition. The present aeroelastic method, that provides a CFD inflow solution instead of using theoretical inflow models, can be a complement to both the traditional aerodynamics/dynamics coupling and CFD/CSD coupling methods.

In the present method, the CFD solver, Cobalt, is used with a blade element model imbedded for the aerodynamic inflow prediction of a helicopter rotor. The elastic structural dynamics of the rotor is studied by using a multibody dynamics analysis tool, DYMORE [3] which uses a finite element based multibody dynamics approach for the analysis of nonlinear elastic multibody systems. In the previous work, the method has been applied to a four-blade articulated model rotor [7]. A comparison of the computed aerodynamic and structural dynamic results with those of theoretical inflow models showed that the current method gives good predictions for aerodynamic performance and dynamic response of a rotor and has the potential to be used for more complex practical situations such as a helicopter hovering in the airwake of a ship.

In this paper, the aeroelastic method is applied to the H-34 helicopter rotor which has been flight [8] and wind tunnel tested [9], and widely used for rotor model validations. A low speed case with advance ratio  $\mu=0.129$  and rotor thrust coefficient  $C_T/\sigma=0.075$  ( $\sigma$  is solidity of the rotor), and a high speed case with advance ratio  $\mu=0.30$  and rotor thrust coefficient  $C_T/\sigma=0.075$  are calculated and discussed. Comparisons are made with flight test data for the blade normal force, the chord and flap bending moments and the torsional moment at several spanwise locations. In the near future, the developed aeroelastic method that integrates the CFD solver Cobalt and DYMORE will be applied to a whole helicopter for a combined aerodynamic and structural dynamic analysis. The integrated solution of the helicopter aerodynamics and the rotor structural dynamic responses will provide an avenue for investigating whether the dynamic unsteady loading of the rotor could be alleviated by actively coupling a rotor control model to the rotor blade motion.

## 2 CFD Inflow Calculation

Cobalt is a parallel, compressible Navier-Stokes flow solver applicable to geometries of arbitrary complexity [10]. Two and three dimensional unstructured grids of arbitrary cell topology are supported along with Overset grids, rigid-body motion, three equations of state, eight turbulence models, and many boundary condition types. Cobalt is fundamentally based on Godunov's first-order accurate, cell-centered, finite volume, exact Riemann solution method. Second-order spatial accuracy is achieved via upwind-biased reconstruction based on least-squares gradients. Stability of the second-order method is ensured by a multi-dimensional TVD limiter. The inviscid flux function, reconstruction, and TVD limiter have been constructed to minimize numerical dissipation while ensuring stability. Viscous terms, computed from the least-squares gradients, are initially formed so as to satisfy conservation and linearity-preservation.

The spatial operator ultimately computes residuals that an implicit temporal operator uses to advance the flow solution in time. The so-called 'left hand side' of the implicit method is constructed with analytical Jacobians and the resulting matrix equation is typically solved with an iterative Gauss-Seidel linear solver (an iterative Jacobi linear solver is used on vector machines). This implicit method is robust and accurate over a wide range of flow conditions. Second-order temporal accuracy and Newton sub-iterations provide accuracy with relatively large time-steps in time-dependent flows. The Wilcox  $k-\omega$  model was used in the present work for the inflow calculations.

With the version of Cobalt used in the Aerodynamics Laboratory of the Institute for Aerospace Research, National Research Council Canada, there are a few options for rotor modeling: actuator disk, annulus and blade element methods. The blade element method applies 2D aerodynamic properties of the rotor blade sections to the rotor disk or annulus. The thrust is calculated from user-provided aerodynamic lift and drag coefficients data, a collective-pitch schedule, geometric data and local flow conditions. The blade element

method was adopted for the current aeroelastic model to provide the rotor inflow conditions.

### **3 Rotor Structural Loads and Airloads**

DYMORE is a finite element based tool for the dynamic analysis of nonlinear elastic multibody systems. The multibody dynamics analysis is cast within the framework of nonlinear finite element methods, and the element library includes rigid and deformable bodies as well as joint elements. Deformable bodies are modeled with the finite element method, in contrast with the classical approach to multibody dynamics that predominantly relies on rigid bodies or introduces flexibility by means of a modal representation. With today's advances in computer hardware, an inexpensive personal computer can provide enough computational power to run full finite element models of complex, nonlinear elastic systems. Hence, resorting to modal reduction in order to save CPU time is no longer a valid argument for most of structural dynamic problems, especially when considering the possible loss of accuracy associated with this simplification.

In DYMORE, the formulations of beams and shells are geometrically exact, i.e. they account for arbitrarily large displacements and finite rotations. The equations of equilibrium are written in a Cartesian inertial frame. Constraints are modeled using the Lagrange multiplier technique. This leads to systems of equations that are highly sparse. DYMORE can treat arbitrarily complex topologies. Furthermore, because it is an extension of the finite element method (FEM) to multibody systems, the algorithms such as sparse solvers, and data structures developed for FEM analyses are directly applicable. A distinguishing feature of multibody systems is the presence of a number of joints that impose constraints on the relative motion of the various bodies of the system. These joints are sufficient to model most configurations. A key element in DYMORE is the development of robust and efficient time integration algorithms to deal with the large scale, nonlinear, differential/algebraic equations resulting from the proposed formulation. Static, dynamic, stability, and trim analyses can be

performed on a DYMORE model. Furthermore, efficient post-processing and visualization tools are available to obtain physical insight into the dynamic response of a DYMORE model.

Simplified models based on lifting line theory and vortex wake models, or high fidelity sophisticated CFD codes can be used for modeling the aerodynamic loads that might be acting on the multibody system. At each time step of the simulation, the aerodynamic loads acting on the system are computed based on the current configuration, and are then used to evaluate the dynamic response. The multibody dynamics procedure can also be coupled with a computational fluid dynamics code [11].

The blade element method based on 2D aerodynamic theory was also integrated with DYMORE which has a few unsteady inflow models. A 3D dynamic inflow model based on the theory for unsteady flow over a circular disk, with a pressure jump across the disk [12], was used here for comparison and validation purposes.

### **4 Results and Discussions**

The H-34 helicopter has an articulated four-bladed rotor. The blade has a radius of 8.5344 m (28 ft), a chord of 0.4167 m (1.367ft) and a blade twist of -8 degree. The cross section is a NACA0012 airfoil. The details of the blade structural properties are given in [8].

The flight test data [8] of an H-34 helicopter have been a benchmark for rotor loads correlation. The blade flap and chord bending and torsional moment data were measured at six radial stations ( $r/R=0.15, 0.275, 0.375, 0.45, 0.575, \text{ and } 0.65$ ), three radial stations ( $r/R=0.15, 0.375 \text{ and } 0.575$ ) and two radial stations ( $r/R=0.15 \text{ and } 0.5$ ), respectively, and were averaged over three consecutive revolutions. Time history data are available with a 15 degree azimuthal increment.

Two flight cases, one low speed and one high speed, were studied in this paper. The trim solution was solved for the controls that yielded the rotor thrust and first harmonic flapping motion to match the measured values with the rotor shaft angle at the measured values.

The blade section normal forces, calculated using a dynamic inflow model and the present CFD inflow model, were compared with the flight data. Comparisons were also made for the blade flap bending, chord bending and torsional moments.

#### 4.1 Low Speed

The flight test number 6 in [8] was selected for this low speed analysis. In this case, the thrust coefficient is 0.075 and the advance ratio is 0.129 (forward speed of 48 knots and the rotor speed of 214 rpm). The blade section normal force is shown in Figs. 1(a)-(c). Both the dynamic inflow model and CFD inflow model give reasonable predicted results in comparison with the flight test data. The dynamic inflow model yields better inboard results in amplitude while the CFD inflow model predicts better near the blade tip as shown in Figs. 2(a)-(c). The blade section vibratory normal force obtained by removing the steady, 1/rev, and 2/rev components is presented in Figs. 1(d)-(f). It is noted that the vibratory normal force is mainly affected by the second flap bending mode which is close to 3/rev. The CFD inflow model

provides better vibratory normal force results in both phase and magnitude.

The calculated and measured flap bending moments are compared in Figs. 3 and 4. While the predictions by both the dynamic and CFD inflow models were not in good agreement with the flight data, the CFD inflow model produced better results in magnitude. For the vibratory flap bending moment, the CFD inflow model also provided marginally better predictions although both models underestimated the magnitude.

Figs. 5 and 6 show the blade chord bending moments. The predicted results are in poor agreement with the flight data. Both inflow models did not capture most of the 3/rev components as shown by the flight data, which was expected in this low speed case where the blade-vortex interactions were important but could not be simulated by both of the inflow models. For the torsional moment as shown in Figs. 7 and 8, the CFD inflow model performed much better than the dynamic inflow model for both vibratory and oscillatory torsional moments which excludes the steady component

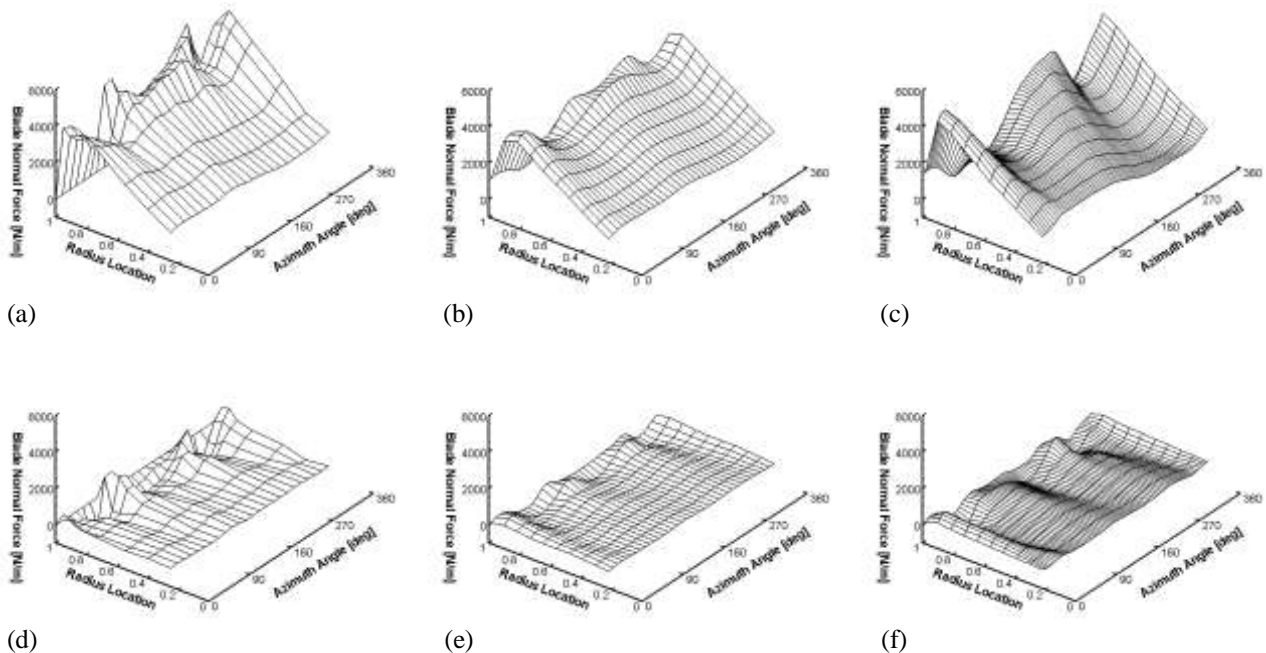


Fig. 1 Calculated and measured blade normal force for the low speed case:  $V=48$  knots, rotor speed=214 rpm. (a) Measured normal force, 0-10 harmonics. (b) Calculated normal force by the dynamic inflow model, 0-10 harmonics. (c) Calculated normal force by the CFD inflow model, 0-10 harmonics. (d) Measured normal force, 3-10 harmonics. (e) Calculated normal force by the dynamic inflow model, 3-10 harmonics. (f) Calculated normal force by the CFD inflow model, 3-10 harmonics

## DEVELOPMENT OF AN AEROELASTIC METHOD FOR PREDICTING ROTOR AIRLOADS AND STRUCTURAL LOADS

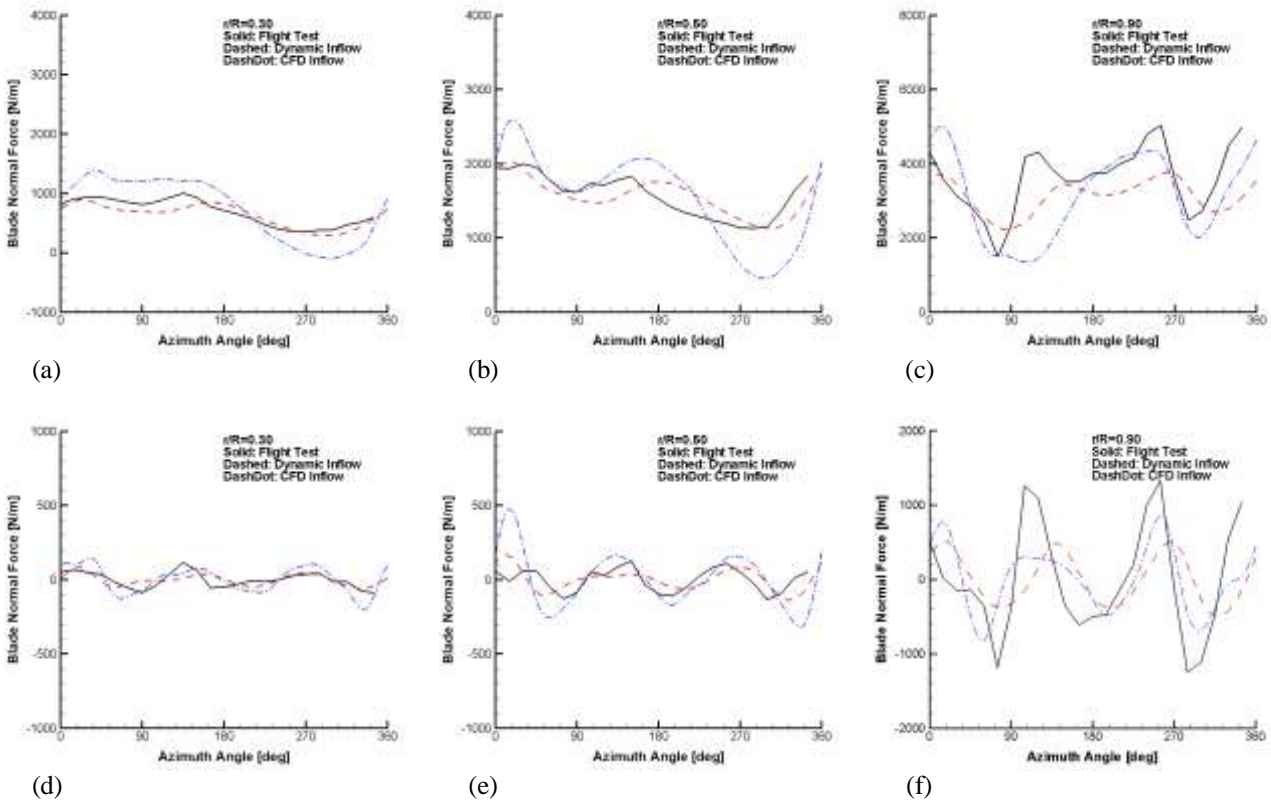


Fig. 2 Calculated and measured blade normal force at three radial locations for the low speed case:  $V=48$  knots, rotor speed=214 rpm. (a)  $r/R=0.30$ , 0-10 harmonics. (b)  $r/R=0.50$ , 0-10 harmonics. (c)  $r/R=0.90$ , 0-10 harmonics. (d)  $r/R=0.30$ , 3-10 harmonics. (e)  $r/R=0.50$ , 3-10 harmonics. (f)  $r/R=0.90$ , 3-10 harmonics

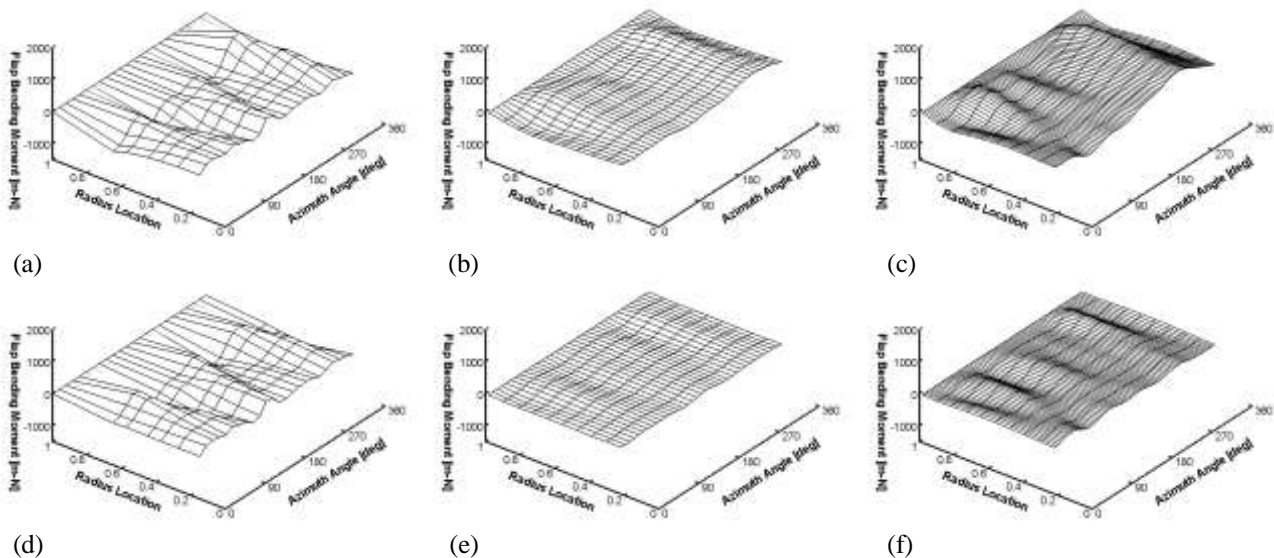


Fig. 3 Calculated and measured blade flap bending moment for the low speed case:  $V=48$  knots, rotor speed=214 rpm. (a) Measured flap bending moment, 1-12 harmonics. (b) Calculated flap bending moment by the dynamic inflow model, 1-12 harmonics. (c) Calculated flap bending moment by the CFD inflow model, 1-12 harmonics. (d) Measured flap bending moment, 3-12 harmonics. (e) Calculated flap bending moment by dynamic inflow model, 3-12 harmonics. (f) Calculated flap bending moment by the CFD inflow model, 3-12 harmonics

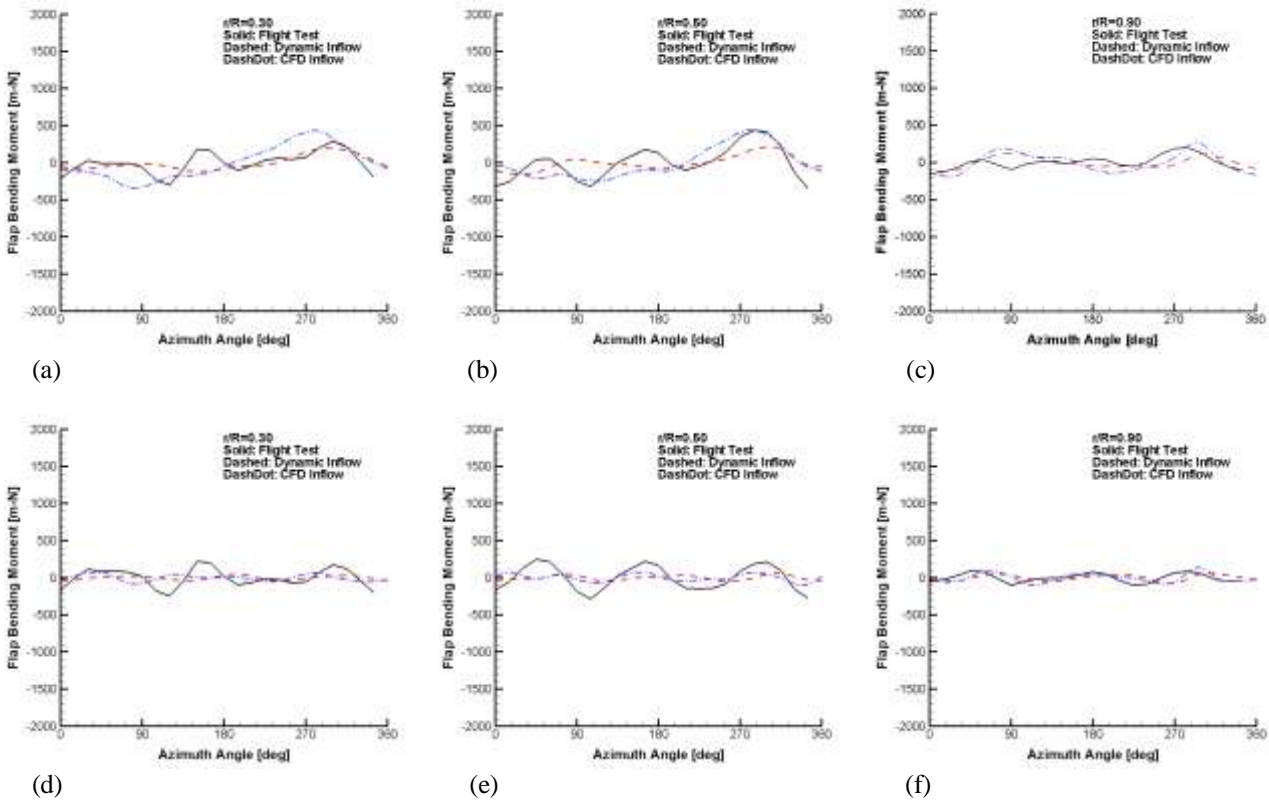


Fig. 4 Calculated and measured blade flap bending moment at three radial locations for the low speed case:  $V=48$  knots, rotor speed= 214 rpm. (a)  $r/R=0.30$ , 1-12 harmonics. (b)  $r/R=0.50$ , 1-12 harmonics. (c)  $r/R=0.90$ , 1-12 harmonics. (d)  $r/R=0.30$ , 3-12 harmonics. (e)  $r/R=0.5$ , 3-12 harmonics. (f)  $r/R=0.9$ , 3-12 harmonics

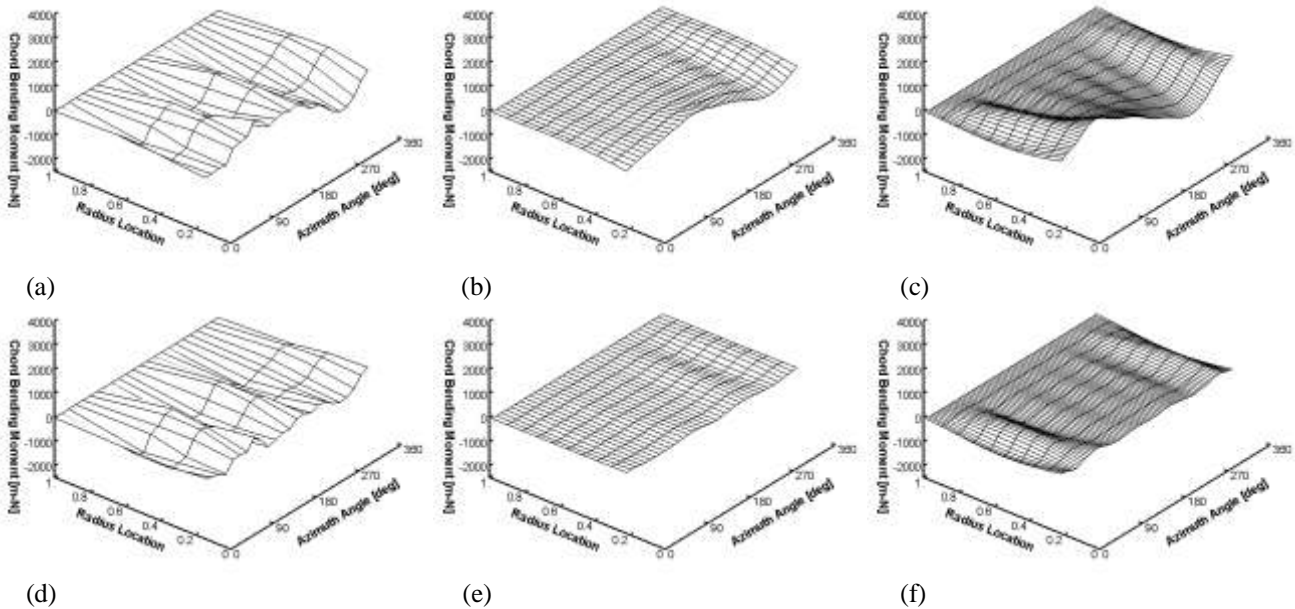


Fig. 5 Calculated and measured blade chord bending moment for the low speed case:  $V=48$  knots, rotor speed=214 rpm. (a) Measured chord bending moment, 1-12 harmonics. (b) Calculated chord bending moment by the dynamic inflow model, 1-12 harmonics. (c) Calculated chord bending moment by the CFD inflow model, 1-12 harmonics. (d) Measured chord bending moment, 3-12 harmonics. (e) Calculated chord bending moment by the dynamic inflow model, 3-12 harmonics. (f) Calculated chord bending moment by the CFD inflow model, 3-12 harmonics

## DEVELOPMENT OF AN AEROELASTIC METHOD FOR PREDICTING ROTOR AIRLOADS AND STRUCTURAL LOADS

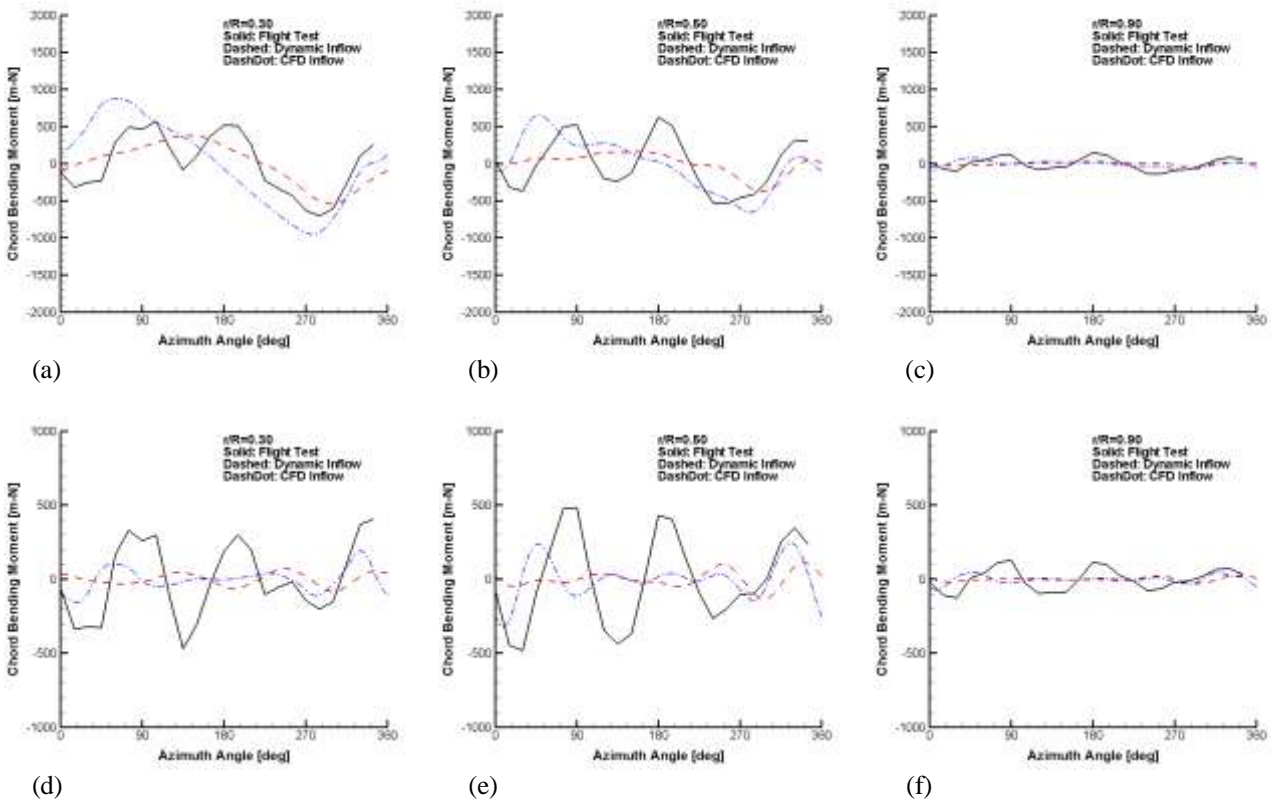


Fig. 6 Calculated and measured blade chord bending moment at three radial locations for the low speed case:  $V=48$  knots, rotor speed= $214$  rpm. (a)  $r/R=0.30$ , 1-12 harmonics. (b)  $r/R=0.50$ , 1-12 harmonics. (c)  $r/R=0.90$ , 1-12 harmonics. (d)  $r/R=0.30$ , 3-12 harmonics. (e)  $r/R=0.5$ , 3-12 harmonics. (f)  $r/R=0.9$ , 3-12 harmonics

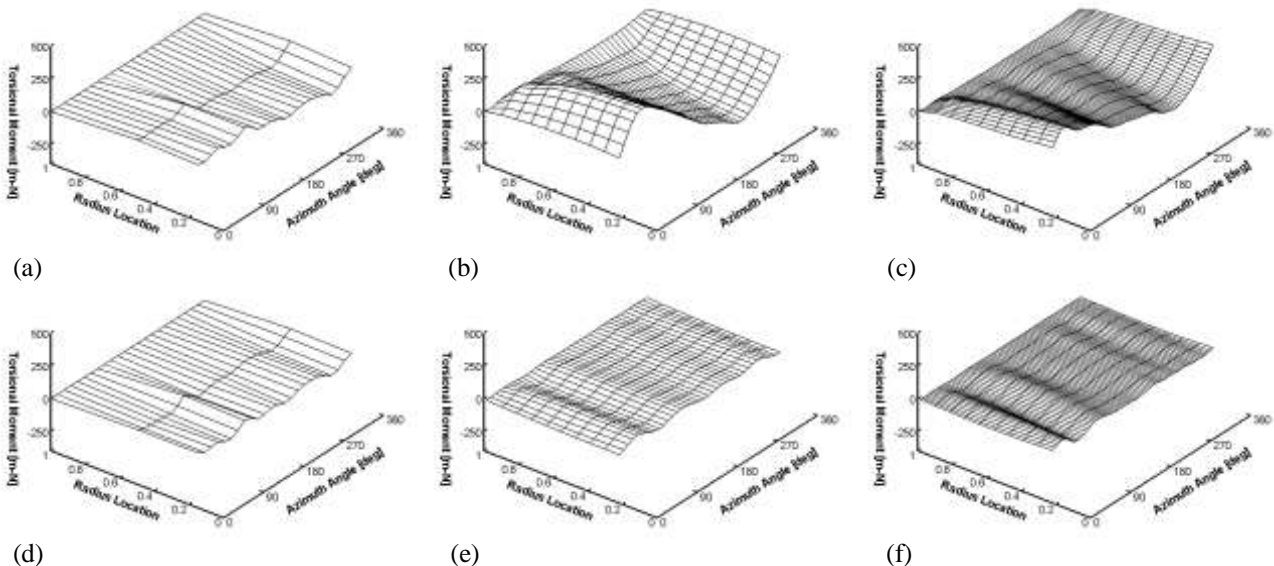


Fig. 7 Calculated and measured blade torsional moment for the low speed case:  $V=48$  knots, rotor speed= $214$  rpm. (a) Measured torsional moment, 1-12 harmonics. (b) Calculated torsional moment by the dynamic inflow model, 1-12 harmonics. (c) Calculated torsional moment by the CFD inflow model, 1-12 harmonics. (d) Measured torsional moment, 3-12 harmonics. (e) Calculated torsional moment by the dynamic inflow model, 3-12 harmonics. (f) Calculated torsional moment by the CFD inflow model, 3-12 harmonics

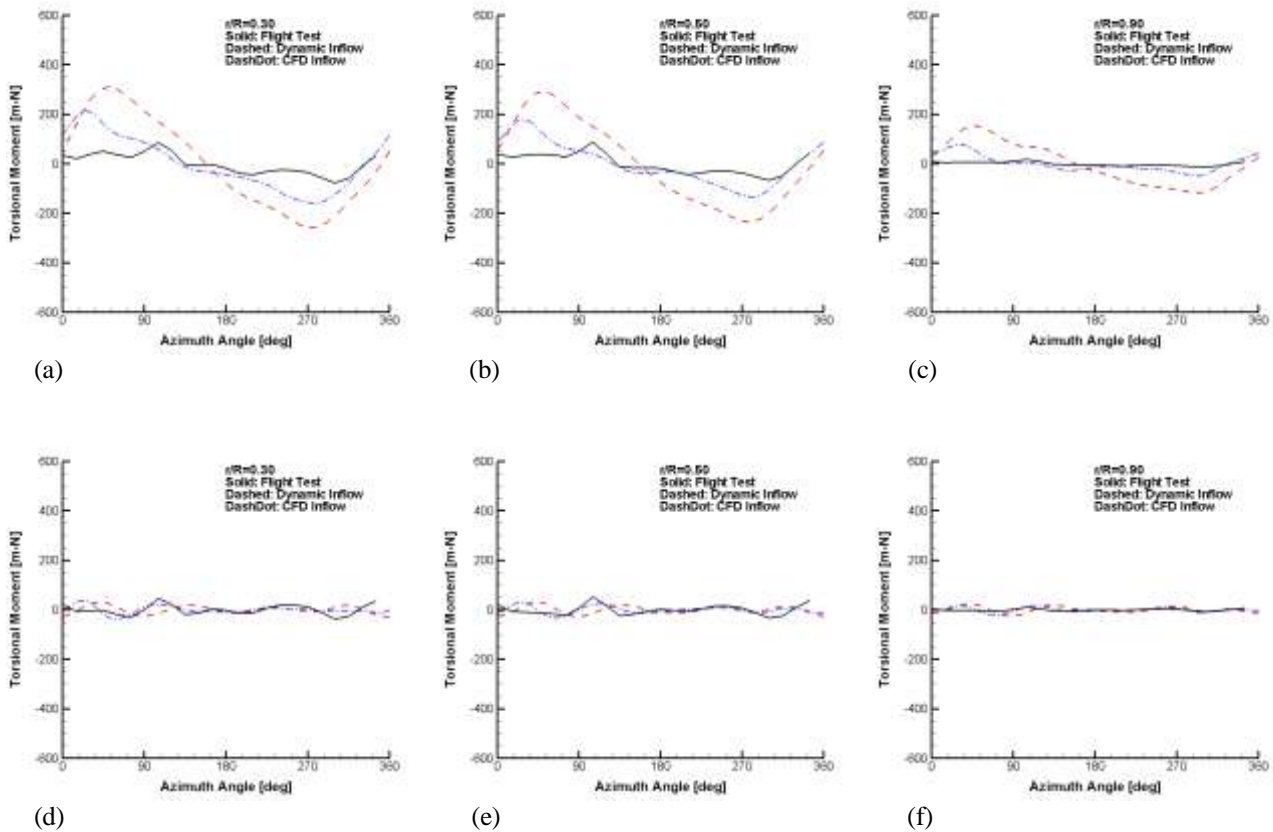


Fig. 8 Calculated and measured blade torsional moment at three radial locations for the low speed case:  $V=48$  knots, rotor speed=214 rpm. (a)  $r/R=0.30$ , 1-12 harmonics. (b)  $r/R=0.50$ , 1-12 harmonics. (c)  $r/R=0.90$ , 1-12 harmonics. (d)  $r/R=0.30$ , 3-12 harmonics. (e)  $r/R=0.5$ , 3-12 harmonics. (f)  $r/R=0.9$ , 3-12 harmonics

## 4.2 High Speed

For the high speed case, the flight test number 18 in [8] was selected. In this case, the thrust coefficient is 0.075 and the advance ratio is 0.30 (forward speed of 112 knots and the rotor speed of 216 rpm). The blade section normal force is shown in Fig 9(a)-(c). Both the dynamic inflow model and CFD inflow model give again reasonable predicted results in comparison with the flight test data. The dynamic inflow model underpredicted the magnitude of the blade normal force while the CFD inflow model overpredicted it.

The calculated and measured flap bending moments are compared in Fig. 10. Relative to the low speed case, the predictions by both the dynamic and CFD inflow models were in reasonable agreement with the flight data. For the vibratory flap bending moment, both inflow models provided good predictions in phase and magnitude.

Fig. 11 shows the blade chord bending moment. The CFD inflow model produced better results than the dynamic inflow model. For the torsional moment, as shown in Fig. 12, both inflow models significantly overpredicted the magnitude although the CFD inflow model yielded better results than the dynamic inflow model.

## DEVELOPMENT OF AN AEROELASTIC METHOD FOR PREDICTING ROTOR AIRLOADS AND STRUCTURAL LOADS

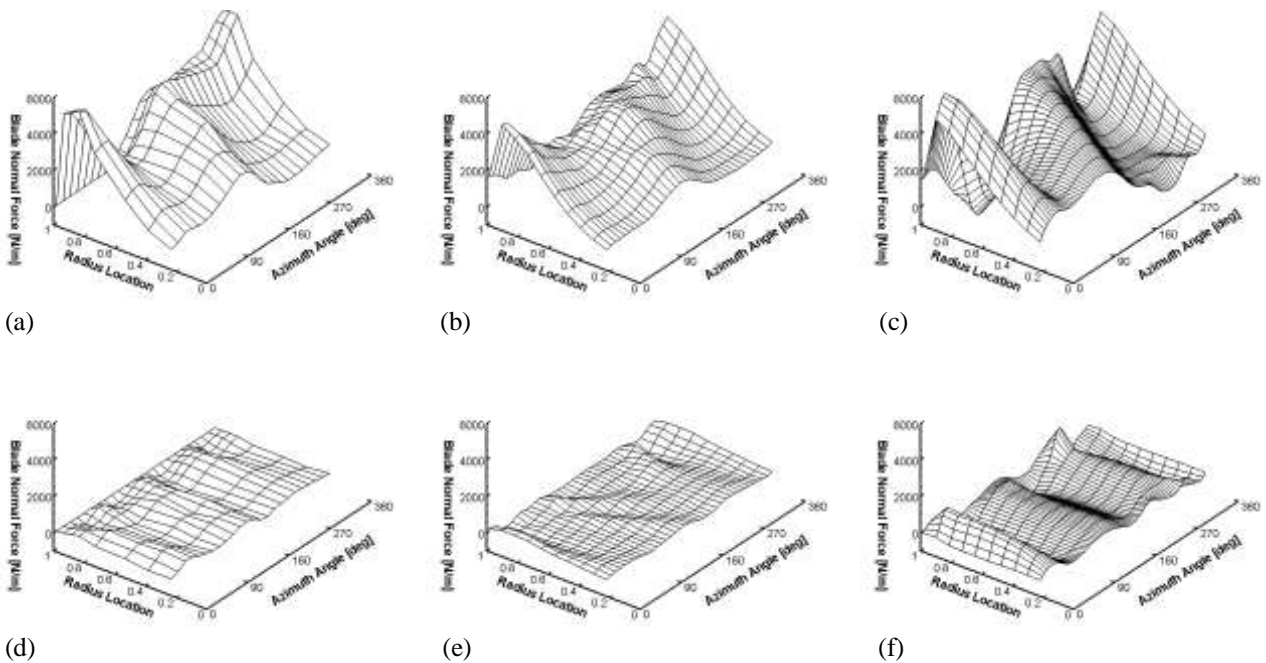


Fig. 9 Calculated and measured blade normal force for the high speed case:  $V=112$  knots, rotor speed= $216$  rpm. (a) Measured normal force, 0-10 harmonics. (b) Calculated normal force by the dynamic inflow model, 0-10 harmonics. (c) Calculated normal force by the CFD inflow model, 0-10 harmonics. (d) Measured normal force, 3-10 harmonics. (e) Calculated normal force by the dynamic inflow model, 3-10 harmonics. (f) Calculated normal force by the CFD inflow model, 3-10 harmonics.

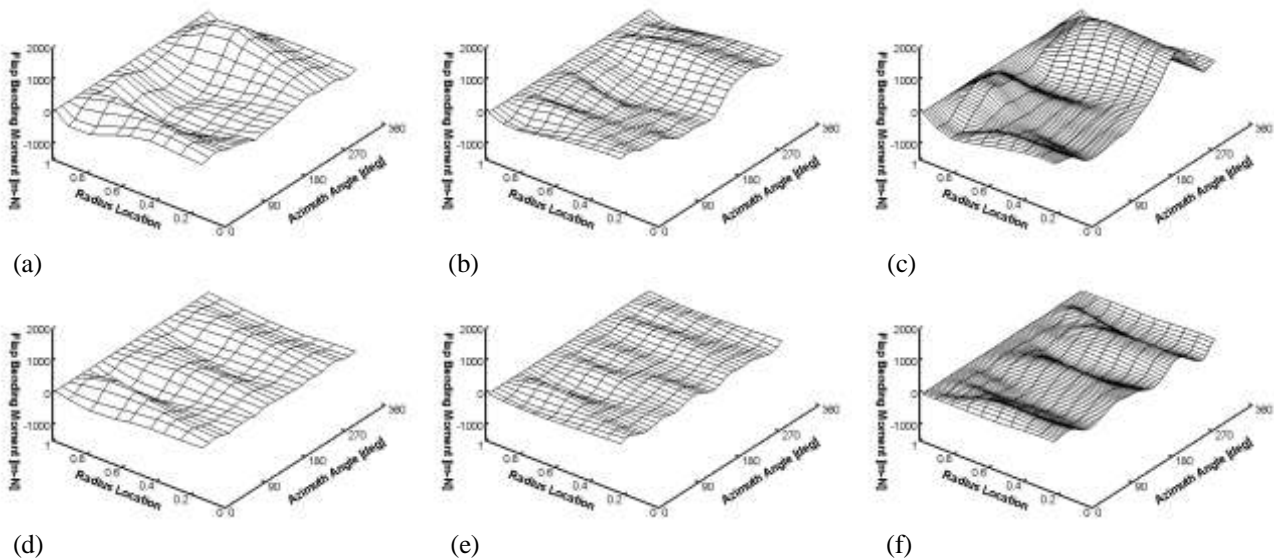


Fig. 10 Calculated and measured blade flap bending moment for the high speed case:  $V=112$  knots, rotor speed= $216$  rpm. (a) Measured flap bending moment, 1-12 harmonics. (b) Calculated flap bending moment by the dynamic inflow model, 1-12 harmonics. (c) Calculated flap bending moment by the CFD inflow model, 1-12 harmonics. (d) Measured flap bending moment, 3-12 harmonics. (e) Calculated flap bending moment by the dynamic inflow model, 3-12 harmonics. (f) Calculated flap bending moment by the CFD inflow model, 3-12 harmonics.

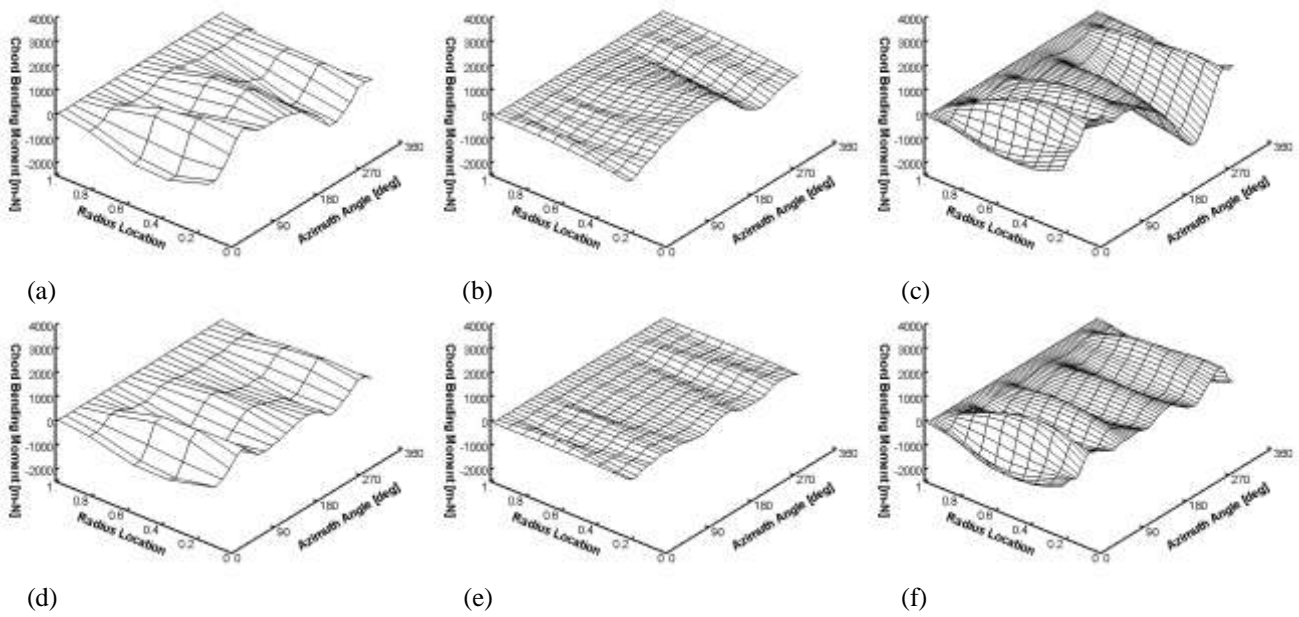


Fig. 11 Calculated and measured blade chord bending moment for the high speed case:  $V=112$  knots, rotor speed= $216$  rpm. (a) Measured chord bending moment, 1-12 harmonics. (b) Calculated chord bending moment by the dynamic inflow model, 1-12 harmonics. (c) Calculated chord bending moment by the CFD inflow model, 1-12 harmonics. (d) Measured chord bending moment, 3-12 harmonics. (e) Calculated chord bending moment by the dynamic inflow model, 3-12 harmonics. (f) Calculated chord bending moment by the CFD inflow model, 3-12 harmonics

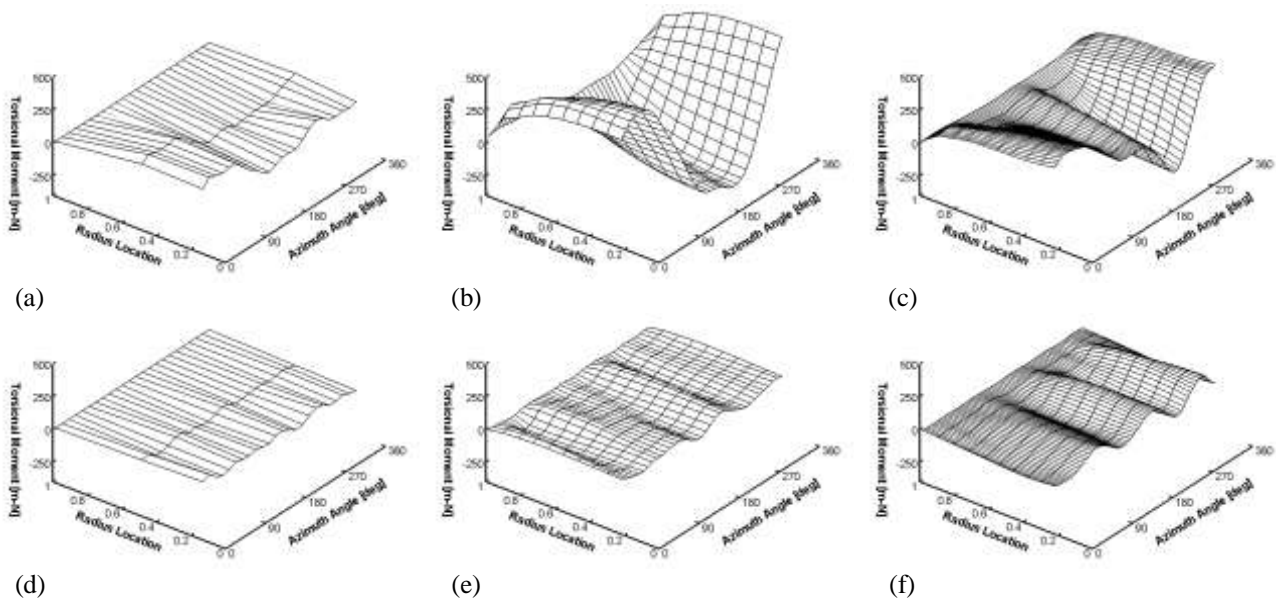


Fig. 12 Calculated and measured blade torsional moment for the high speed case:  $V=112$  knots, rotor speed= $216$  rpm. (a) Measured torsional moment, 1-12 harmonics. (b) Calculated torsional moment by the dynamic inflow model, 1-12 harmonics. (c) Calculated torsional moment by the CFD inflow model, 1-12 harmonics. (d) Measured torsional moment, 3-12 harmonics. (e) Calculated torsional moment by the dynamic inflow model, 3-12 harmonics. (f) Calculated torsional moment by the CFD inflow model, 3-12 harmonics

## 5 Conclusions

An aeroelastic method has been developed by integrating the CFD solver Cobalt with the

comprehensive flexible multibody dynamic system tool DYMORE. The method has been applied to the four-bladed articulated rotor H-34. The analysis indicated that the model could produce reasonable results for the rotor

aerodynamic normal force and blade section flap bending moment. Cobalt's capability in predicting the inflow information over a rotor should make the model applicable to a much more complex physical situations such as a helicopter hovering in the airwake of a ship.

However, in general, both the dynamic inflow and CFD inflow models are not satisfactory in predicting the chord bending and torsional moments. The current CFD inflow model is not iterated with DYMORE dynamic solution. It is expected that such iteration should improve the inflow results and thus the overall dynamic and aerodynamic prediction. While the free wake models may provide further improvement in both aerodynamic and dynamic predictions, especially near the blade tip, the CFD/CSD coupling method is the ultimate solution for the rotor dynamics and aerodynamics.

## 6 Acknowledgments

The authors would like to acknowledge the Department of National Defense of Canada for funding this work in a multi-year collaborative project. Thanks also go to the authors' colleague Dr. A. Benmeddour for his comments and suggestions.

## References

- [1] Johnson W. Rotorcraft aerodynamics models for a comprehensive analysis. *54<sup>th</sup> Annual Forum of the American Helicopter Society*, Washington DC, May 20-22, 1998.
- [2] Bir G, Chopra I and Nguyen K. Development of UMARC (University of Maryland Advanced Rotor Code). *American Helicopter Society 46<sup>th</sup> Annual Forum Proceedings*, Washington, D.C., May 1990.
- [3] Bauchau O A and Kang H K. A multibody formulation for helicopter structural dynamic analysis. *Journal of the American Helicopter Society*, Vol. 38, No. 2, April 1993.
- [4] Potsdam M, Yeo H and Johnson W. Rotor airloads prediction using loose aerodynamic/structural coupling. *The American Helicopter Society 60<sup>th</sup> Annual Forum*, Baltimore, MD, June 7-10, 2004.
- [5] Dietz M, Kramer E, Wagner S and Altmikus A. Active rotor performance investigations using CFD/CSD weak coupling. *The 33<sup>rd</sup> European Rotorcraft Forum*, Kazan, Russia, September 11-13, 2007.
- [6] Bielawa R L. *Rotary wing structural dynamics and aeroelasticity*. AIAA Education Series, 2006
- [7] Su J C and Zhang F. An aeroelastic model for helicopter rotors in hover and forward flight conditions. *Canadian Aeronautics and Space Institute AERO'09 Conference*, Kanata, Ontario, May 5-7, 2009.
- [8] Scheiman J. A tabulation of helicopter rotor-blade differential pressures, stresses, and motions as measured in flight. *NASA TM X-952*, 1964.
- [9] Rabbott J P Jr, Lizak A A and Paglino V M. A presentation of measured and calculated full-scale rotor blade aerodynamic and structural loads. *USAAVLABS TR 66-31*, 1966.
- [10] Strang W Z, Tomaro R F and Grismer M J. The defining methods of Coalt60: a parallel, implicit, unstructured Euler/Navier-Stokes flow solver. *AIAA paper 99-0786*.
- [11] Murty H, Bottasso C L, Dindar M, Shephard M S and Bauchau O A. Aeroelastic analysis of rotor blades using nonlinear fluid/structure coupling. *The American Helicopter Society 53<sup>rd</sup> Annual Forum*, Virginia Beach, VA, April 1997.
- [12] Peters D A and He C J. Finite state induced flow models. Part II: three-dimensional rotor disk. *Journal of Aircraft*, Vol. 32, No. 2, pp323-333, 1995.

## Contact Author Email Address

Jichao.Su@nrc-cnrc.gc.ca

## Copyright Statement

The authors confirm that they, and/or their company or organization, hold copyright on all of the original material included in this paper. The authors also confirm that they have obtained permission, from the copyright holder of any third party material included in this paper, to publish it as part of their paper. The authors confirm that they give permission, or have obtained permission from the copyright holder of this paper, for the publication and distribution of this paper as part of the ICAS2010 proceedings or as individual off-prints from the proceedings.